Electronic Supplementary Information (ESI)

Knowledge-based development of a nitrate-free synthesis route for Cu/ZnO methanol synthesis catalysts via formate precursors

by
Malte Behrens, Stefan Kißner, Frank Girsgdies, Igor Kasatkin, Felix Hermerschmidt, Katharina Mette, Holger Ruland, Martin Muhler, and Robert Schlögl

Experimental Details

Characterization

XRD: The samples were measured on a STOE STADI P transmission diffractometer equipped with a primary focusing Ge monochromator (Cu Kα_1 radiation) and a linear position sensitive detector (moving mode, step size 0.1°, counting time 10 s/step, resolution 0.01°, total accumulation time 634 s). The samples were mounted in the form of a clamped sandwich of small amounts of powder fixed with a small amount of grease between two layers of thin polyacetate film.

Rietveld refinement: Refinements were done in the 2θ range 5–80° using the software package TOPAS [S1]. The background was modelled using a third order Chebychev polynomial. Some technical details are listed in the following table.

Zn content x	0	0.04	0.10	0.15	0.21
R_{exp} [a]	0.0674	0.0666	0.0660	0.0700	0.0693
R_{wp} [a]	0.1000	0.0942	0.0993	0.0936	0.0799
R_p [a]	0.0718	0.0682	0.0713	0.0672	0.0586
R_{exp}' [a]	0.1080	0.1101	0.1016	0.1271	0.1435
R_{wp}' [a]	0.1601	0.1556	0.1528	0.1701	0.1655
R_p' [a]	0.1446	0.1414	0.1319	0.1577	0.1602
GOF	1.48	1.41	1.50	1.34	1.15
R_{Bragg}	0.04035	0.02689	0.02376	0.02773	0.02006
No. of reflections	160	160	159	161	164
No. of parameters	32	32	32	32	32
FHI database ID#	8141	8000	7975	8639	8059

[a] Primed *R* values are background corrected; definition of the R values according to [S2].

Electron microscopy: SEM images were taken in a Hitachi S-4800 (FEG) system. HRTEM images were taken on a Philips CM200FEG microscope operated at 200 kV. The coefficient of spherical aberration was $C_s = 1.35$ mm. The information limit was better than 0.18 nm allowing the principal phases to be identified in HRTEM images. High-resolution images with a pixel size of 0.016 nm were taken at the magnification of 1083000× with a CCD camera.

Elemental analysis: Cu to Zn ratios of the samples were obtained by X-ray fluorescence (XRF) measurements. The samples were glassed with $Li_2B_4O_7$ and analyzed in a Bruker S4 Pioneer X-ray spectrometer.

Synthesis

Materials

ZnO (>99.99%) and $Cu_2(OH)_2CO_3$ (p.a.) were obtained from Aldrich, Na_2CO_3 (>99.9%), and formic acid (85%, p.a.) from Roth, and NaOH (p.a.) from Riedel de Häen.

Highly crystalline model precursors:

In course of the preparation, constant pH co-precipitation was performed in an automated laboratory reactor (Mettler-Toledo Labmax, 2 L, prefilled with 400 mL water) at T = 65 °C and pH 5.5 from aqueous 1.6 M Na_2CO_3 solution and aqueous 0.5 M Cu,Zn solution. The latter was prepared by dissolving appropiate amounts of $Cu_2(OH)_2CO_3$ and ZnO in a solution of conc. formic acid (85 %) and water. Solidification of the metal ions was incomplete and the analytical Cu:Zn ratios determined by XRF (100:0, 96:4, 90:10, 85:15 and 78:22) were always higher than the nominal ones (100:0, 75:25, 50:50, 35:65, 25:75). The precipitate was thoroughly washed with water and finally dried at 60 °C for 16 hours. Calcination was performed in a flow of pure O_2 at 200 °C for 3 hours (heating rate: 2 Kpm). Temperature programmed reduction to activate the catalyst took place in TPDRO 1100 instrument at 200°C for 3 hours (heating rate: 1 Kpm) in 5% H_2/Ar.

Catalyst precursors:

The preparation matches the method described above for the highly crystalline model precursors, but applying T = 25 °C, pH = 7 and NaOH instead of Na_2CO_3. The increase in pH leads to a more complete precipitation and the deviation between nominal and analytical Cu:Zn ratio was could be significantly lowered (75:25 vs. 81:19).

Anion composition:

While the Cu:Zn ratio of the precursors has been determined by XRF, the anionic composition of a $Cu_2(OH)_3HCO_2$ sample was investigated by IR spectroscopy as

described in reference [13] of the main text. The results confirmed the presence of OH-groups and formate (1579 cm^{-1}), while carbonate was absent. The overall cation-to-anion ratio was checked by TGA. The mass loss at 500 °C in air is 28.9% in very good agreement with the theoretical mass loss of 28.7% if CuO is assumed as the only decomposition product.

Catalytic testing / Cu surface area determination

Catalytic testing was performed in a flow set-up equivalent to that described in ref. [S3]. For fast on-line gas analysis, a calibrated quadrupole mass spectrometer (Pfeiffer Vacuum, Thermostar) was used. The following gases of high purity were used: He (99.9999 %), H_2 (99.9999 %), N_2O/He (1% N2O, 99.9995 %), H_2/He (2.0 % H_2, 99.9999%) and a mixture of 72% H_2, 10% CO, 4% CO_2 in He used as methanol synthesis feed gas (99.9995 %). A glass-lined stainless steel microreactor was filled with 100 mg catalyst (sieve fraction 250-355 μm). The catalyst was reduced by heating to 175 °C (1 K min^{-1}) in a gas mixture of 2.0 % H_2/He and subsequently in 100% H_2 to 240 °C. The catalytic activity under steady-state conditions was determined at 220°C and at 10 bar pressure, using a flow rate of 50 N ml min^{-1}. The copper surface area was determined applying N_2O reactive frontal chromatography according to the method proposed by Chinchen et al. [S4] at somewhat more moderate reaction conditions [S3]. The catalytic test was performed at 220 °C and 10 bar pressure.

Results

XRD refinements

The monoclinic basic copper nitrate $Cu_2(OH)_3NO_3$ is a well-known compound and the crystal structure was originally described in the space group $P2_1/m$ [S5]. Later works conclusively proved the symmetry to be $P2_1$ [S6,S7]. However, the lower symmetry is caused mainly by the position of the terminal oxygen atoms of the nitrate ligand and the hydrogen atoms, while the majority of the structure is pseudo-symmetric. For the sake of a more stable Rietveld refinement, we thus decided to derive a structure model for $(Cu_{1-x}Zn_x)_2(OH)_3HCO_2$ from the corresponding nitrate structure in $P2_1/m$ [S5] replacing the symmetric $-NO_2$ residue with a disordered $-C=O$ group (hydrogen positions were not considered). It turned out that besides the terminal oxygen atom also the carbon atom of the formate group has to be desribed with a statistically occupied split position. The final model is thus analogous to the structure of the nitrite derivative $Cu_2(OH)_3NO_2$ [S8]. Finally, we should mention that a single crystal investigation on $Cu_2(OH)_3HCO_2$ has been published during the work on this paper [S9] indicating that the true symmetry of $Cu_2(OH)_3HCO_2$ (and thus the zinc substituted series) is most probably $P2_1$ in analogy to the monoclinic nitrate.

Table of refined lattice parameters of $(Cu_{1-x}Zn_x)_2(OH)_3HCO_2$, space group $P2_1/m$)

x	0	0.04	0.10	0.15	0.21
a / Å	5.59522(9)	5.58401(12)	5.56789(13)	5.55317(15)	5.53641(16)
b / Å	6.06594(9)	6.08624(12)	6.11275(14)	6.14171(16)	6.17023(17)
c / Å	6.94190(14)	6.94037(19)	6.9407(2)	6.9414(3)	6.9444(3)
β / °	105.8484(13)	105.3705(17)	104.7695(19)	104.133(2)	103.5526
V / Å^3	226.654(7)	227.436(9)	228.421(10)	229.576(12)	230.619(12)

Graphical representation of Rietveld fit

Figure S1: Rietveld fit of the highly crystalline model precursor $x = 0$ (data points: experimental data; red line: theoretical pattern; green tick marks: position of Bragg reflections; black line: difference curve). The quality of this fit is representative for all refinements.
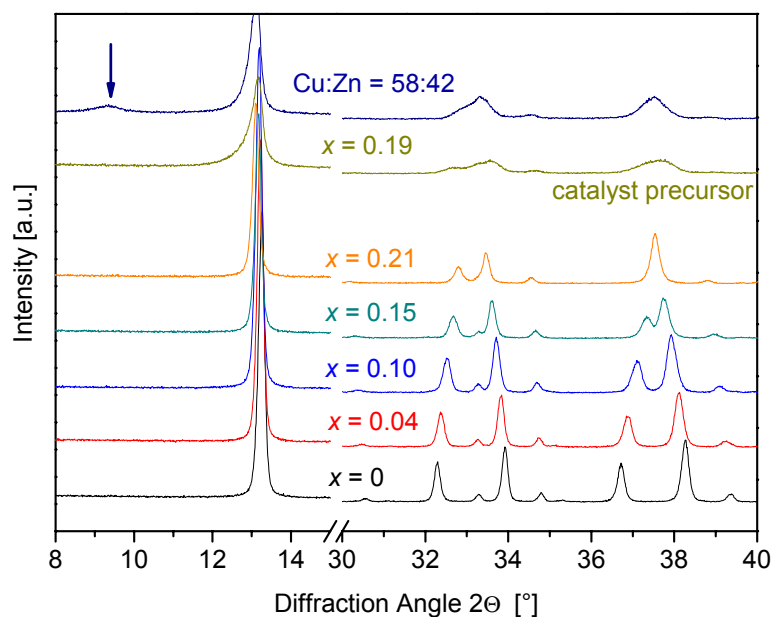
XRD patterns as a function of Zn-content

Figure S2: XRD of formate precursors with different Cu:Zn ratios showing systematic shifts in the peak positions and the appearance of an unidentified by-phase (arrow) for Zn contents > 0.21

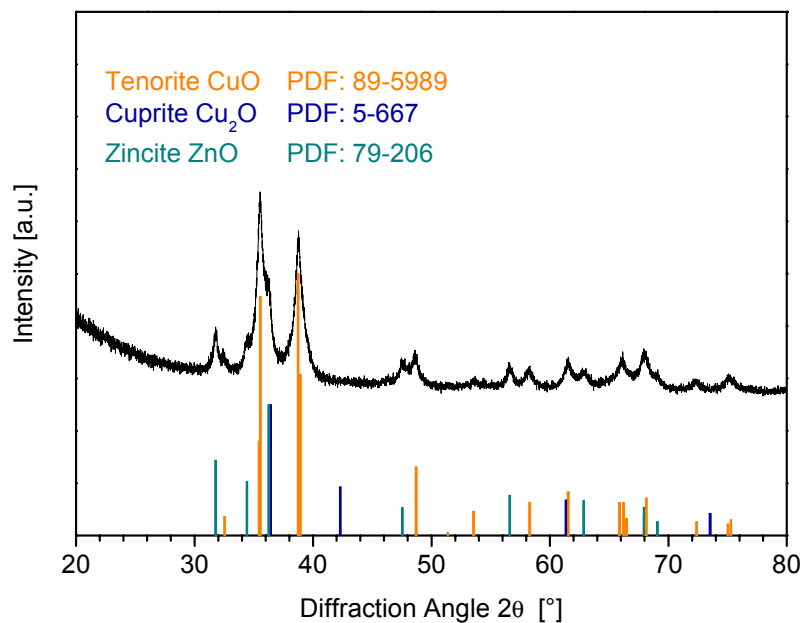*XRD of calcined sample $(Cu_{0.79}Zn_{0.21})_2(OH)_3HCO_2$*

Figure S3: XRD shows the presence of CuO and ZnO after thermal decomposition in O_2 (black line: experimental data; orange columns: tenorite; blue columns: cuprite; turquoise columns: zincite; FHI database ID #8176)
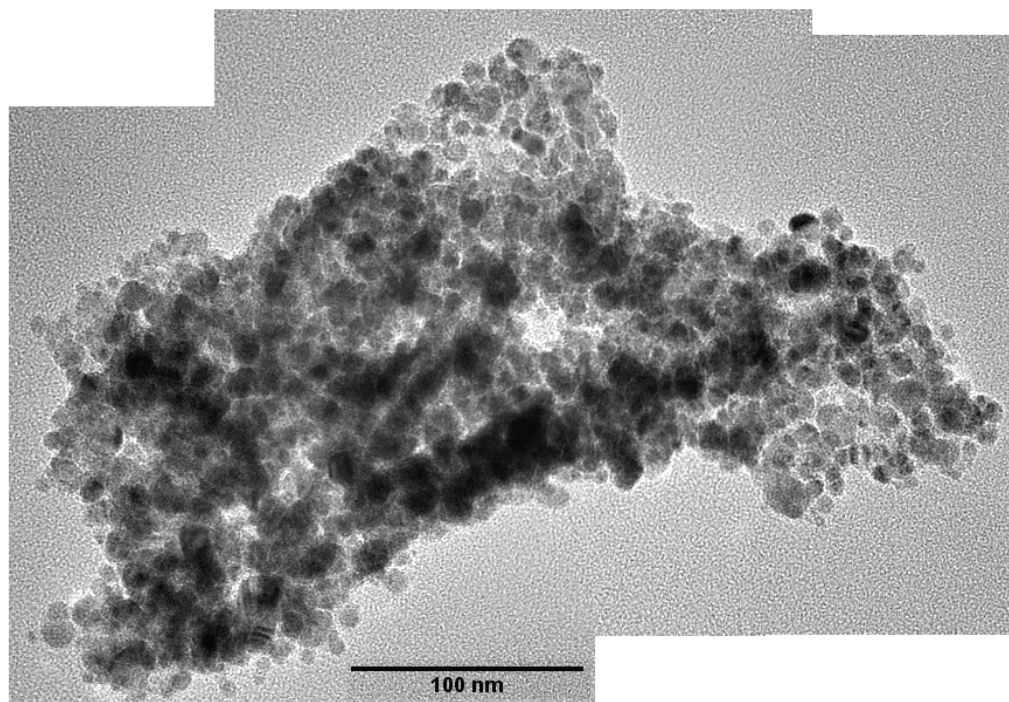
TEM investigations

Figure S4: Low resolution image of a nanoparticluate Cu/ZnO aggregate obtained after calcination and reduction of a $(Cu_{0.81}Zn_{0.19})_2(OH)_3HCO_2$ catalyst precursor
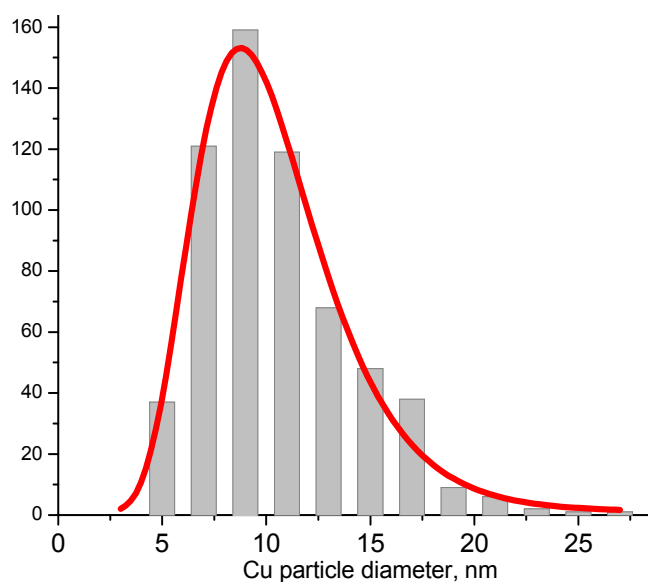

Figure S5: Corresponding Cu particle size distribution determined by TEM based on 609 particles. Mean diameter is 10.5 nm (standard deviation: 3.6 nm, standard error: ± 0.1 nm, distribution skewness: 0.95, distribution kurtosis: 1.05). The mean volume weighted diameter is 11.7 nm;

References

[S1]   A. A. Coelho, *Topas, General Profile and Structure Analysis Software for Powder Diffraction Data*, Version 3.0, Bruker AXS GmbH, Karlsruhe, Germany, **2006**.

[S2]   R. A. Young in *The Rietveld Method*, ed. R.A. Young, Oxford University Press **1993**, 1 ff.

[S3]   O. Hinrichsen, T. Genger, M. Muhler, *Chem. Eng. Technol.* **2000**, 23, 956-959.

[S4]   G. C. Chinchen, C. M. Hay, H. D. Vanderwell, K. C. Waugh, *J. Catal.* **1987**, 103, 79.

[S5]   N. Nowacki, R. Scheidegger, *Helv. Chim. Acta* 1952, **35**, 375.

[S6]   H. Effenberger, *Z. Kristallogr.* 1983, **165**, 127.

[S7]   N. Guillou, M. Louër, D. Louër, *J. Solid State Chem.* 1994, **109**, 307.

[S8]   M Schmidt, H. Möller, H. D. Lutz, Z. Anorg. Allgem. Chem. 1993, **619**, 1287.

[S9]   H. Euler, B. Barbier, A. Kirfel, S. Haseloff, G. Eggert, *Z. Kristallogr.* 2009, **224**, 609.